

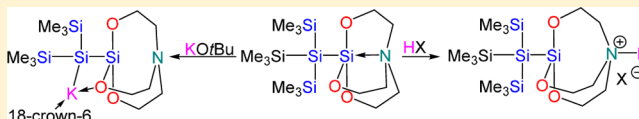
Oligosilanylsilatrane

Mohammad Aghazadeh Meshgi,[†] Judith Baumgartner,[‡] and Christoph Marschner^{*,†}

[†]Institut für Anorganische Chemie der Technischen Universität Graz and [‡]Institut für Chemie, der Karl Franzens Universität Graz, Stremayrgasse 9, 8010 Graz, Austria

S Supporting Information

ABSTRACT: Oligosilanes with attached silatranyl units were obtained by reactions of potassium oligosilanides with a silatranyl triflate. Interaction between Si and N atoms was observed in the ²⁹Si NMR spectra (upfield-shifted SiO₃ resonances) and in the solid-state structures (Si–N distances between 2.29 and 2.16 Å). The Si–N interaction can be “switched off” either by protonation of the nitrogen lone pair or by potassium silanide formation caused by trimethylsilyl group cleavage in the presence of potassium *tert*-butoxide.



INTRODUCTION

Due to the four valence electrons that group 14 elements possess, they exhibit a strong prevalence for tetravalent compounds. However, even for carbon, compounds with both diminished (lower) and higher coordination sphere are known. As carbon is a rather small atom, hypervalent coordination states usually lead to steric interactions between substituents. Therefore, such situations are typically not stable but only represent intermediates or transition states, such as in S_N2 reactions.^{1–3}

For the heavier elements silicon, germanium, and tin the situation is somewhat different. While they share the electronic situation of carbon, their atomic radii are larger and therefore they can more easily accommodate additional substituents. Today, numerous stable penta- and hexacoordinate compounds are known for silicon,^{4–8} germanium,^{7–9} and tin.^{10–12} In particular, the so-called atrane molecules (silatrane, germa-trane, and stannatrane), substances which feature the heavy group 14 element with a trialkanolamine ligand N–[(CR¹R²)_nO]₃ER (E = Si, Ge), have been studied to quite some extent. In many cases it was found that hypercoordination has a profound influence on the bond located trans to the nitrogen atom.

Interestingly, a survey of known sila- and germatranes with different triethanolamine substituents reveals that, despite the large variety of attached groups R which have been studied, almost no compounds of atranes with bonds to other heavy group 14 elements exist.^{13,14} Only very recently Zaitsev et al. published a first study addressing compounds where an atrane unit is attached to a heavy group 14 oligomer unit.¹⁵ In the current account we want to present our activities concerning the synthesis and chemistry of silatranyl-substituted oligosilanes.

RESULTS AND DISCUSSION

In recent years we have put some effort into the investigation of conformational properties of oligosilanes.^{16–20} In particular, compounds with bulky end groups such as the tris(trimethylsilyl)silyl unit were found to exhibit a strong

preference for transoid arrangements of chains. This conformation is of some importance, as it is known to facilitate the delocalization of σ-bonding electrons.²¹ In addition to conformational properties, also electronic factors such as substituent electronegativity^{22–26} and hypercoordination^{27,28} can influence the optical absorption properties. We therefore were interested in introducing silyl substituents into oligosilanes, which have a weakened Si–Si bond.

Synthesis. One issue that has to be dealt with when hypercoordinate entities are incorporated into oligosilanes is the choice of which group should be used. We decided that the plain silatrane consisting of a silicon atom with a triethanolamine ligand would serve best as a starting point.

In principle there are two ways to prepare a silatranyl-substituted oligosilane. Either the silatrane silicon atom is introduced first and then the triethanolamine unit is attached or the silatranyl unit is prepared first and is then attached as a whole to the oligosilane. After some experiments we found both strategies possible but concentrated on the second one, which proved to be more general and gave better yields in our hands.

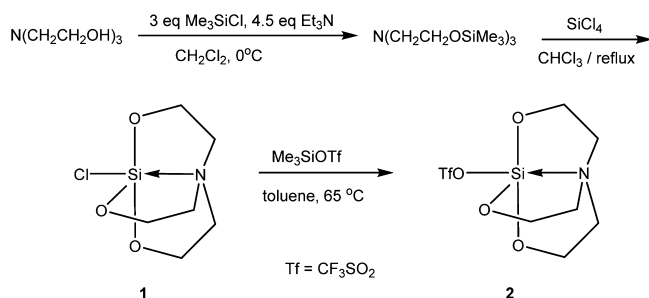
For the attachment of the silatrane unit the obvious way to proceed seemed to be reaction of a silatrane with a suitable leaving group with a silanyl anion. While we found that reactions with silatranyl chloride **1** are a possible option, it turned out that the use of the respective triflate **2** gave better yields. Synthesis of silatranyl triflate **2** was accomplished by reaction of silatranyl chloride²⁹ **1** with trimethylsilyl triflate (Scheme 1).³⁰

Reaction of silatranyl triflate **2** with tris(trimethylsilyl)silyl potassium³¹ gave the expected neopentasilane **3** in an acceptable yield of 51% (Scheme 2). In an analogous way also the related compounds **4** and **5** were obtained.

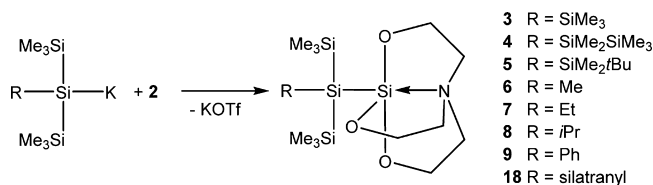
With the reaction of isotetrasilanides and **2** being established, the question arose whether 2-trisilanides would also react the same way. During the course of our studies on oligosilanyl

Received: May 12, 2015

Scheme 1. Synthetic Access to Silatranyl Triflate 2



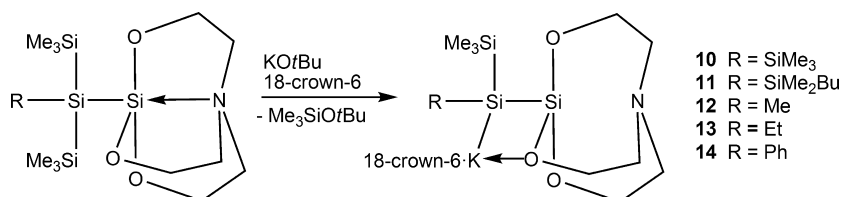
Scheme 2. Formation of Oligosilanylsilatrane using Salt Elimination Reactions



anions, on several occasions the reactivity of 2-trisilanides differed substantially from that of isotetrasilanides.³² However, for the case of the reactions with 2, the use of a series of 2-trisilanides occurred smoothly. Reaction of 2 with methylbis-(trimethylsilyl)silyl potassium gave 6 in a respectable yield of 75%, reflecting the better steric accessibility of the silanide (Scheme 2). With sterically more demanding silanides carrying ethyl, isopropyl, and phenyl the reactions also proceeded to 7–9; however, these reactions gave less satisfying yields (Scheme 2).

Given the access to this series of oligosilanylsilatrane, we wanted to find out whether these compounds could be used as building blocks. Therefore, compound 3 was reacted with potassium *tert*-butoxide to cleanly obtain compound 10, which is the product of trimethylsilyl abstraction (Scheme 3). An analogous reaction was carried out with compound 5 to give 11. In every case attack of the butoxide was selective for a trimethylsilyl group. When the same reaction was attempted with the alkylated oligosilanylsilatrane 6 and 7, again the expected silatranyl silanides 12 and 13 were formed. However, in these cases the reactions were not as clean and also attack at the silatranyl unit was observed, yielding the bis(trimethylsilyl)-alkylsilyl potassium species and the silatranyl *tert*-butyl ether as side products. For the methylated substrate 6 the ratio between the silanide 12 and the silatranyl ether was about 2:1, whereas for the sterically somewhat better shielded ethylated compound 7 the ratio of 13 to the silatranyl ether was about 8:1. The phenylated compound 9, however, displayed a clean reaction with potassium *tert*-butoxide to selectively afford silanide 14.

Scheme 3. Formation of Silatranyl Oligosilanides by Trimethylsilyl Abstraction

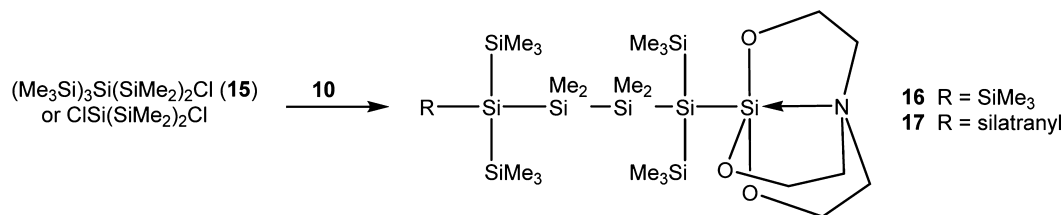


For a proper comparison of the UV-absorption properties of oligosilanes with and without silatranyl units it was desirable to obtain derivatives of 2,2,5,5-tetrakis(trimethylsilyl)-decamethylhexasilane.²⁰ Reaction of the respective silanide (Me₃Si)₃Si(Me₂Si)₂Si(K)(SiMe₃)₂^{33,34} with 2 did not proceed to 16 with a satisfactory yield due to the increased steric bulk of the anion. However, reaction of the anion 10, which was already substituted with silatranyl, with 1-chloro-3,3-bis-(trimethylsilyl)heptamethyltetrasilane 15¹⁹ allowed the isolation of compound 16 (Scheme 4). Following the same strategy, the 2,5-disilatranylhexasilane compound 17 was obtained by reaction of 2 equiv of 10 with 1,2-dichlorotetramethyldisilane (Scheme 4). Although silanide 10 is sterically more demanding than tris(trimethylsilyl)silyl potassium it can react with another equivalent of 2 to give neopentasilane 18 containing two silatranyl units (Scheme 2).

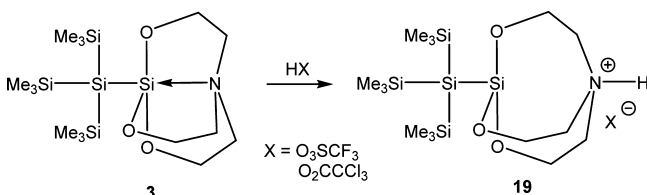
The fact that the silatrane nitrogen atom donates electron density to the silicon diminishes its basicity. For a number of silatrane, in particular ones with electronegative substituents, it has been shown that protonation occurs preferentially at one of the oxygen atoms, which also exhibit a stronger kinetic basicity.^{35,36} Theoretical calculations predict, however, that for a silylated silatrane protonation should occur preferentially at the nitrogen atom.³⁵ To estimate the degree of the nitrogen donation on the Si–Si bond of 3, it was treated with trifluoromethanesulfonic acid to protonate the nitrogen lone pair and thus switch off the Si–N interaction. The obtained ammonium salt 19•OTf forms cleanly and the shut-off Si–N interaction is visible in the NMR spectra and the solid-state structure (Scheme 5). While protonation with the extremely strong trifluoromethanesulfonic acid (pK_a = −14)³⁷ could be expected, an attempt to achieve protonation with excess acetic acid (pK_a = 4.76)³⁷ failed completely. Reaction of 3 with trichloroacetic acid (pK_a = 0.65)³⁷ was not complete with a stoichiometric amount of Cl₃CCO₂H, but a 5-fold excess gave 19•TCA. Other than an osmium complex with a silatranyl ligand,^{38,39} 19•OTf seems to be the only structurally characterized example of a silatrane protonated at the nitrogen atom.

NMR Spectroscopy. The compounds of this study were characterized by multinuclear NMR spectroscopy (Table 1). The proton spectra of the neutral compounds (3–9, 16–18) in CDCl₃ exhibit the typical pattern of two triplets (³J_{H–H} = 5.6 Hz) for the two methylene groups of the silatrane unit with chemical shifts of ca. 3.65 ppm for the O–CH₂ units and 2.72 ppm for the neighboring N–CH₂ moieties. It is interesting to note that a relatively strong solvent effect is observed for the proton spectra, which shall be exemplified for compound 3, for which the methylene resonances OCH₂/CH₂N were found at 3.65/2.72 ppm in CDCl₃ and 3.30/1.83 ppm in C₆D₆. The respective ¹³C resonances of the neutral compounds, which are also all very similar, were found around 58.5 ppm for the O–CH₂ and 51.9 ppm for the N–CH₂ units (in both CDCl₃ and

Scheme 4. Synthesis of Larger Silatranylated Oligosilanes 16 and 17



Scheme 5. Protonation of Silatrane 3 with Trifluoromethanesulfonic Acid or Trichloroacetic Acid



C₆D₆). For the silyl anions 10–14 (in C₆D₆) the proton resonances shift considerably to lower field to values around 3.80 ppm for the methylene groups attached to oxygen atoms and 2.84 ppm for the amino-substituted atoms. The anionic compounds exhibit also slightly diminished coupling constants between the methylene groups. As can be expected, ²⁹Si NMR spectroscopy provides the most direct insight into the electronic situation of the compounds involved in this study (Table 1).

To understand the influence exerted by the nitrogen atom on the silicon atom in the silatranyl unit, comparison with the chemical shift of a related trialkoxysilylated oligosilane is required. The chemical shift of the MeO₃Si group of (MeO₃Si)₄Si⁴⁰ is −35 ppm, and thus the more shielded chemical shift of ca. −53 ppm found for 3–5, 16, and 17 should reflect the degree of hypercoordination (interaction between Si and N). The respective chemical shifts of compounds 6–9, with more electronegative alkylsilyl substituents, are further shifted to values close to −57 ppm, thus

reflecting a stronger degree of hypercoordination, which is consistent with what is observed in the solid-state structures (vide infra). Silatrane, where the attached silyl group bears only methyl and phenyl groups such as Me₃Si, Me₂PhSi, and MePh₂Si,¹³ which are less electron donating than the (Me₃Si)₂SiR groups reported here, allow an even higher degree of hypercoordination and therefore shift even further upfield to values of −64.0, −67.0, and −69.0 ppm, respectively.¹³ Interestingly, the chemical shift for the geminal disilatranylsilane 18 of −46.8 ppm indicates a substantially diminished degree of hypercoordination. The chemical shift of the respective resonance of 19 at −22.8 ppm shows the effect of a silatranyl unit with Si–N interaction turned off by protonation of the nitrogen lone pair. For the silyl anions 10–14 a downfield shift of the silatranyl resonance can be expected. Indeed, a shift from −52.6 ppm for 3 to −11.8 ppm for the respective anion 10 is observed, which reflects not only the expected downfield shift of a silyl group in a position α to a negatively charged atom but also the fact that the Si–N interaction is turned off in these compounds, as is also clearly visible in the solid-state structures (vide infra). Another point worth mentioning is that the ²⁹Si NMR resonances of the negatively charged silicon atoms in compounds 10 (−210.5 ppm) and 11 (−215.7 ppm) appear at considerably higher field in comparison to (Me₃Si)₃SiK (−191.1 ppm).⁴¹ Compounds 11 and 14 are chiral silanides, and 11 is particularly interesting, as the *tert*-butyldimethylsilyl group has two diastereotopic methyl groups which allow determination of the configurational stability of the chiral silanide. Given the additional coordination

Table 1. NMR Spectroscopic Data of Oligosilanyl Silatrane

compd	²⁹ Si				¹³ C OCH ₂ /CH ₂ N	¹ H OCH ₂ /CH ₂ N
	SiMe ₃	SiO ₃	Si _q	other		
3	−9.9	−52.6	−133.9		58.6/52.2 ^a 58.6/51.5 ^b	3.65/2.72 ^a 3.30/1.83 ^b
4	−9.3	−54.0	−132.2	−15.0, −40.0	58.4/51.9 ^a	3.66/2.73 ^a
5	−9.7	−51.5	−136.8	4.0 (tBuMe ₂ Si)	58.7/52.1 ^a	3.65/2.72 ^a
6	−12.9	−57.8	−88.0		58.3/51.8 ^a	3.69/2.74 ^a
7	−13.2	−56.6	−78.4		58.3/51.9 ^a	3.66/2.71 ^a
8	−13.5	−56.6	−69.6		58.5/52.0 ^a	3.67/2.73 ^a
9	−13.1	−56.6	−76.2		58.1/51.6 ^a	3.75/2.76 ^a
10	−3.2	−11.8	−210.5		61.0/54.3 ^b	3.86/2.84 ^b
11	−3.0	−11.0	−215.7	11.3	61.0/54.2 ^b	3.81/2.82 ^b
12	−5.1	−14.9	−144.0		60.9/54.2 ^b	3.76/2.80 ^b
13	−6.2	−15.0	−125.1		61.0/54.3 ^b	3.88/2.88 ^b
14	−7.7	−19.4	−113.0		61.1/54.2 ^b	3.84/2.81 ^b
16	−9.2/−9.6	−53.8	−128.6/−129.3	−30.6/−30.8 (Me ₂ Si),	58.5/51.8 ^a	3.66/2.73 ^a
17	−9.2	−53.2	−129.5	−31.2	58.8/51.5 ^b	3.36/1.90 ^b
18	−9.5	−46.8	−135.5		59.4/52.7 ^b	3.68/2.71 ^b
19	−9.7	−22.8	−141.1		56.4/53.1 ^b	3.34/2.64 ^b

^aMeasured in CDCl₃. ^bMeasured in C₆D₆.

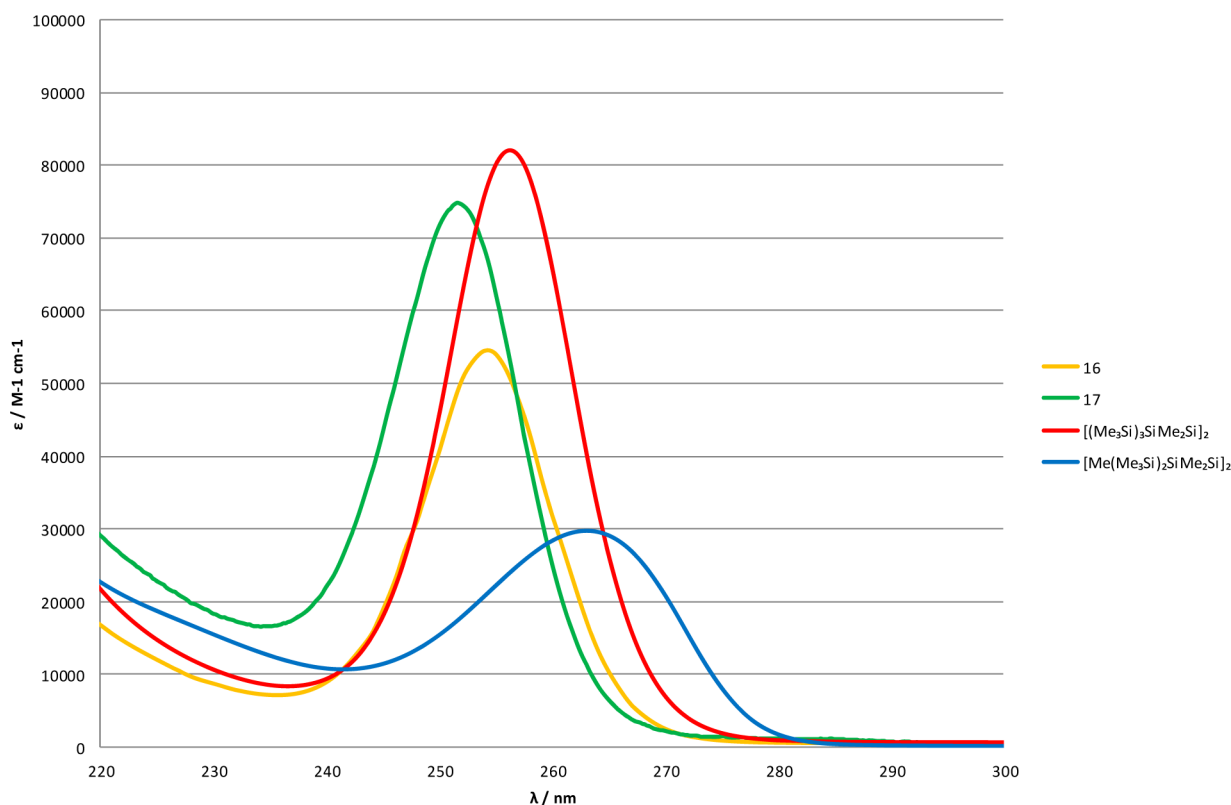


Figure 1. UV spectra of compounds **16** and **17** and of $[(\text{Me}_3\text{Si})_3\text{SiMe}_2\text{Si}]_2$ and $[\text{Me}(\text{Me}_3\text{Si})_2\text{SiMe}_2\text{Si}]_2$ in pentane.

to the silatranyl oxygen, an increased configurational stability might be possible. However, at ambient temperature two different methyl resonances could not be observed either in the ^1H or in the ^{13}C NMR spectrum. Therefore, it has to be concluded that at room temperature pyramidal inversion of silanide **11** is fast on the NMR time scale.

UV Spectroscopy. The UV absorption spectra of the silatranes **3**, **5**–**9**, and **18** exhibit the expected absorption bands associated with the trisilane segment around 210 nm only as badly recognizable shoulders. Compound **4**, containing a tetrasilane unit, showed an absorption maximum at 223 nm. For a meaningful comparison to other oligosilanes it is essential to have compounds with well-resolved absorption bands and a number of compounds with similar structures. Compounds **16** and **17**, with one and two silatranyl units, meet these requirements and are therefore best suited to estimate the influence of the silatranyl units on the property of σ -bond electron delocalization. In order to compare these to structurally related compounds UV spectra of 2,2,5,5-tetrakis-(trimethylsilyl)decamethylhexasilane⁴² and 2,5-bis-(trimethylsilyl)dodecamethylhexasilane³³ are also shown in Figure 1.

In the branched oligosilanes with hexasilane units as the longest chain segments the effect of the silatranyl units in comparison to that of trimethylsilyl groups is not very pronounced. For compound **16**, containing one silatranyl group, the longest wavelength absorption band (254 nm) shows a 2 nm hypsochromic shift. The same band is shifted further toward blue by another 2 nm for compound **17**. While the molecular structure of **17** in the solid state indicates the silatranyl units as part of the all-transoid hexasilane conformer, it needs to be pointed out that for **16** and **17** in solution rotation of the bulky tris(silyl)silyl group is likely to be facile

and therefore all-transoid hexasilane conformers with trimethylsilyl end groups are presumably contributing to the hexasilane absorption band.

Conversely, for 2,5-bis(trimethylsilyl)-dodecamethylhexasilane, where two trimethylsilyl groups are exchanged for methyl groups, the hexasilane band shows a bathochromic shift of 7 nm to an absorption maximum of 263 nm. This behavior is consistent with the typically observed trend of electron-withdrawing substituents causing a bathochromic shift of the absorption maxima and electron-donating groups being responsible for contrasting behavior.⁴³

Crystal Structure Analysis. Compounds **3**, **5**–**7**, **9**–**11**, **14**, and **17**–**19** of this study were subjected to single-crystal XRD analysis. For compound **3** (Figure 2) it was found to be impossible to conduct the measurement at 100 K, as the crystals at this temperature lost structural integrity. At 200 K the structure was solved in the triclinic space group $P\bar{1}$.

Crystals of the more asymmetric compound **5** (Figure 3) were not sensitive to low temperature and crystallize in the trigonal space group $R\bar{3}$. Both trimethylsilyl groups and also the *tert*-butyldimethylsilyl group showed some disorder. The methylated and ethylated isotetrasilanes **6** (Figure 4) and **7** (Figure 5) both crystallize in the orthorhombic space group $Pcca$, with the latter compound exhibiting somewhat elongated axes. For **7** some disorder of the ethyl CH_3 group can be found. The phenylated compound **9** (Figure 6) crystallizes in the orthorhombic space group $Pca2_1$ with two crystallographically independent molecules in the asymmetric unit. The silanides **10** (Figure 7) and **11** (Figure 8) both crystallize in the monoclinic space group $P2_1/n$. For compound **10** some disorder in the silatranyl unit was found. For the phenylated silanide **14** (Figure 9), crystallizing in the triclinic space group $P\bar{1}$, an additional benzene molecule was found in the

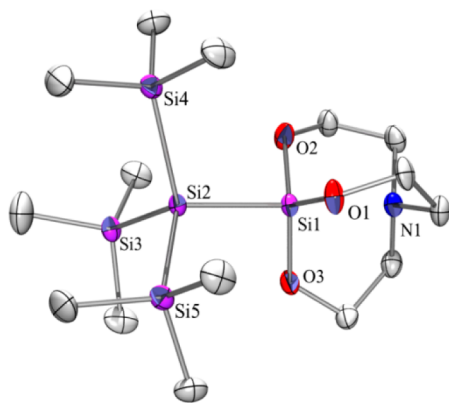


Figure 2. Molecular structure of **3** (thermal ellipsoid plot drawn at the 30% probability level). All hydrogen atoms are omitted for clarity. Selected bond lengths (in Å) and angles (in deg): Si(1)–O(1) 1.650(3), Si(1)–N(1) 2.292(4), Si(1)–Si(2) 2.3509(18), Si(2)–Si(3) 2.3351(18), Si(3)–C(13) 1.863(5), N(1)–C(1) 1.462(6), N(1)–C(5) 1.461(5), O(1)–C(2) 1.420(5), C(1)–C(2) 1.522(6); C(1)–N(1)–C(5) 114.4(4), C(2)–O(1)–Si(1) 123.4(3), C(4)–O(2)–Si(1) 123.9(3), C(6)–O(3)–Si(1) 123.6(3).

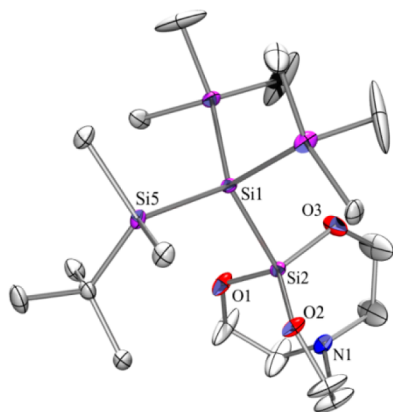


Figure 3. Molecular structure of **5** (thermal ellipsoid plot drawn at the 30% probability level). All hydrogen atoms are omitted for clarity. Selected bond lengths (in Å) and angles (in deg): Si(5)–C(13) 1.883(7), Si(5)–Si(1) 2.3510(18), Si(6)–C(23) 1.885(7), Si(1)–Si(4) 2.3456(12), Si(1)–Si(2) 2.346(1), Si(2)–O(1) 1.661(2), Si(2)–N(1) 2.283(3), O(1)–C(2) 1.376(4), N(1)–C(1) 1.446(5), C(1)–C(2) 1.393(5); O(3)–Si(2)–O(2) 117.55(15), O(3)–Si(2)–O(1) 116.97(15), O(2)–Si(2)–O(1) 117.83(12), C(5)–N(1)–C(1) 114.4(4).

asymmetric unit. Compound **17** (Figure 10) crystallizes in the monoclinic space group $P2_1/c$ with two crystallographically independent half-molecules in the asymmetric unit, for which the second halves are generated by a center of inversion. Also for **17** a disordered silatranyl unit was found. The disilatrane **18** (Figure 11) crystallizes in the monoclinic space group $C2/c$. The silatranyl triflate **19** (Figure 12), which crystallizes in the monoclinic space group $P2_1/c$, shows three crystallographically independent ion pairs in addition to half a molecule of benzene on a special position in the asymmetric unit. The hydrogen attached to the nitrogen atom of **19** was detected in the experimental electron density map.

The number of structures determined in the course of this study allows a fair assessment of the influence of the silatranyl unit on the oligosilane structure. The most important structural

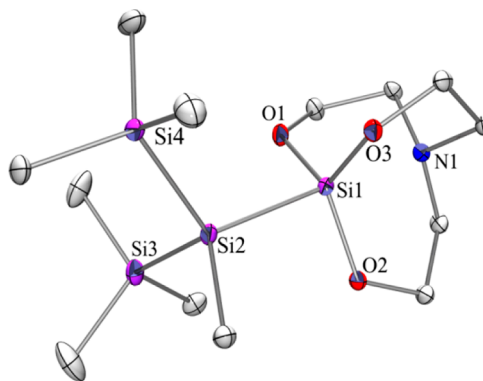


Figure 4. Molecular structure of **6** (thermal ellipsoid plot drawn at the 30% probability level). All hydrogen atoms are omitted for clarity. Selected bond lengths (in Å) and angles (in deg): Si(1)–O(3) 1.670(2), Si(1)–O(1) 1.673(2), Si(1)–O(2) 1.682(2), Si(1)–N(1) 2.167(3), Si(1)–Si(2) 2.3523(13), Si(2)–C(7) 1.908(3), Si(3)–C(8) 1.871(4), N(1)–C(1) 1.474(4); O(3)–Si(1)–O(1) 117.43(12), O(1)–Si(1)–O(2) 120.09(12), C(1)–N(1)–C(4) 113.7(2).

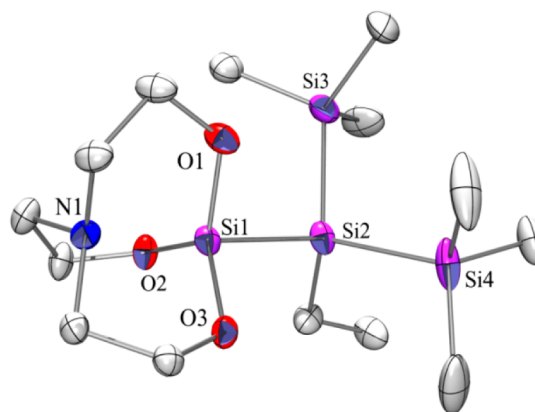


Figure 5. Molecular structure of **7** (thermal ellipsoid plot drawn at the 30% probability level). All hydrogen atoms are omitted for clarity. Selected bond lengths (in Å) and angles (in deg): Si(1)–O(1) 1.671(3), Si(1)–N(1) 2.182(3), Si(1)–Si(2) 2.3443(15), Si(2)–C(7) 1.907(4), Si(2)–Si(4) 2.3341(17), N(1)–C(2) 1.473(5), O(1)–C(1) 1.409(5); O(1)–Si(1)–O(3) 117.49(14), O(1)–Si(1)–O(2) 120.03(15), O(1)–Si(1)–N(1) 82.58(13), Si(4)–Si(2)–Si(1) 113.38(6), C(6)–N(1)–C(4) 114.1(3).

values with respect to this are the Si–N distance and the bond between the silatranyl unit and the oligosilane (Table 2).

For the chlorosilatrane **1** the Si–N distance has been determined to be 2.023 Å.⁵ For the isotetrasilanyl-substituted compounds **3** (Figure 2) and **5** (Figure 3) elongated distances of 2.293(3) and 2.283(2) Å consistent with the more electron donating and sterically much more demanding character of the attached silyl substituents were found. For compounds **6** (Figure 4), **7** (Figure 5), and **9** (Figure 6) the smaller size of the attached group but also its more electronegative character of the alkyl and aryl substituents cause a shortening of the Si–N distances to values of 2.167(3), 2.182(4), and 2.162(5) Å. The respective value for a PhMe_2Si -substituted silatrane was found to be even shorter: 2.153(2) Å.¹³

The Si–SiO₃ distances of **3**, **5**–**7**, and **9** are 2.351(2), 2.346(1), 2.352(1), 2.344(2), and 2.383(2) Å, respectively, which are rather typical Si–Si bond lengths observed in oligosilanes. Along with the silanide formation, which causes a localization of negative charge on the silicon atom trans to the

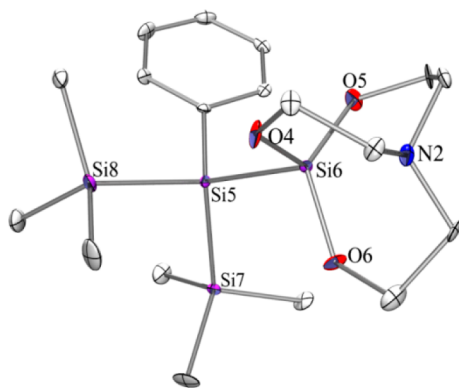


Figure 6. Molecular structure of **9** (thermal ellipsoid plot drawn at the 30% probability level). All hydrogen atoms are omitted for clarity. Selected bond lengths (in Å) and angles (in deg): Si(1)–C(3) 1.910(6), Si(1)–Si(4) 2.342(2), Si(5)–Si(6) 2.383(2), Si(5)–C(9) 1.904(6), Si(6)–O(4) 1.662(5), Si(6)–O(6) 1.674(5), Si(6)–O(5) 1.682(5), Si(6)–N(2) 2.176(6), N(1)–C(26) 1.496(8), N(2)–C(32) 1.486(8), O(1)–C(25) 1.430(8); O(4)–Si(6)–O(6) 119.7(3), O(4)–Si(6)–O(5) 118.4(3), O(6)–Si(6)–O(5) 117.3(3), C(36)–N(2)–C(32) 114.2(5).

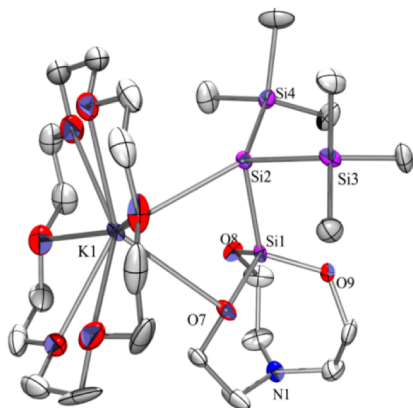


Figure 7. Molecular structure of **10** (thermal ellipsoid plot drawn at the 30% probability level). All hydrogen atoms are omitted for clarity. Selected bond lengths (in Å) and angles (in deg): O(7)–Si(1) 1.659(4), O(7)–K(1) 3.197(5), O(8)–C(15) 1.407(7), O(8)–Si(1) 1.684(4), Si(1)–Si(2) 2.3080(18), Si(2)–K(1) 3.3634(16), N(1)–C(16) 1.430(7); Si(1)–O(7)–K(1) 97.9(2), C(14)–N(1)–C(16) 119.9(6), C(14)–N(1)–C(17) 122.1(6), C(16)–N(1)–C(17) 117.4(5).

nitrogen, an interaction between silicon and nitrogen is no longer observable in compounds **10**, **11**, and **14**. The Si–N distances are between 3.10 and 3.18 Å. Along with this shut-off Si–N interaction Si–SiO₃ bond distances of 2.308(2), 2.295(1), and 2.3088(8) Å for **10**, **11**, and **14** are substantially shorter than those in the neutral compounds **3**, **5**, and **9**, indicating nondisturbed Si–Si bonds. The structural motif of the silanides **10**, **11**, and **14** is different from the usual potassium silanide crown ether complexes. Typically the position of the potassium atom in the solid-state structure is that of a tetrahedral substituent. Complexes **10**, **11**, and **14** show a distortion of the potassium position in order to coordinate to one of the silatrane oxygen atoms. A similar coordination situation was observed for the case of (Me₃Si)₂Si(K)OMe.⁴⁴ This coordination behavior is taken to an extreme by Krempner's silanides (MeOMe₂Si)₃SiK⁴⁵ and (MeOCH₂CH₂OMe₂Si)₃SiK,⁴⁶ where the potassium ion only

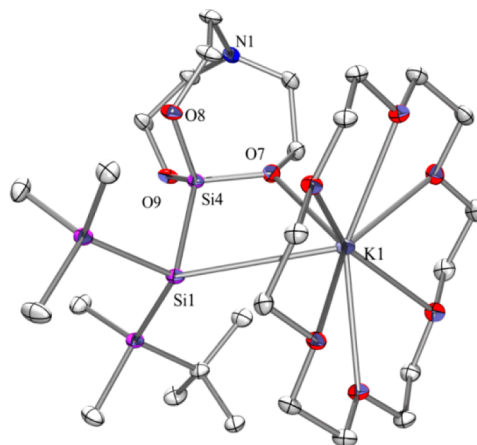


Figure 8. Molecular structure of **11** (thermal ellipsoid plot drawn at the 30% probability level). All hydrogen atoms are omitted for clarity. Selected bond lengths (in Å) and angles (in deg): Si(1)–Si(4) 2.2947(12), Si(1)–Si(2) 2.3276(13), Si(1)–Si(3) 2.3391(14), Si(1)–K(1) 3.6321(13), Si(2)–C(19) 1.878(4), Si(4)–O(8) 1.656(2), Si(4)–K(1) 3.8618(15), O(5)–C(8) 1.430(3), N(1)–C(18) 1.430(4); O(8)–Si(4)–O(9) 105.61(12), O(8)–Si(4)–O(7) 106.14(12), Si(1)–K(1)–Si(4) 35.49(2), C(18)–N(1)–C(14) 119.8(3).

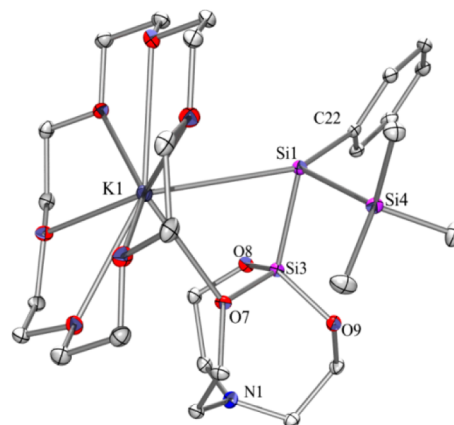


Figure 9. Molecular structure of **14** (thermal ellipsoid plot drawn at the 30% probability level). All hydrogen atoms are omitted for clarity. Selected bond lengths (in Å) and angles (in deg): Si(1)–C(22) 1.9141(17), Si(1)–Si(3) 2.3087(7), Si(1)–K(1) 3.5722(9), Si(3)–O(9) 1.6642(12), Si(4)–C(19) 1.8841(19), K(1)–O(7) 2.9983(12), N(1)–C(16) 1.441(2), O(1)–C(1) 1.421(2); O(9)–Si(3)–K(1) 145.02(5), C(16)–N(1)–C(18) 120.35(14), C(16)–N(1)–C(13) 119.81(14), C(18)–N(1)–C(13) 119.59(14), Si(3)–O(7)–K(1) 111.86(5).

coordinates to the alkoxy groups. However, the Si–K distances of **10**, **11**, and **14** are comparable to what was observed for (Me₃Si)₃SiK-18-crown-6⁴¹ and also the distances between potassium and the silatrane oxygen are only slightly elongated in comparison to K–O distances of the crown ether. The structural properties of compound **17** were expected to be close to those of **3** and **5**. However, the Si–N distances of the two crystallographically independent molecules of **17** are 2.223(4) and 2.209(4) Å and thus are significantly shorter, while the Si–SiO₃ bond distances are comparable to those of **3** and **5**. The two independent molecules exhibit all-transoid hexasilane conformations, with the silatrane silicon atoms being starting and ending points of this particular conformational subunit.

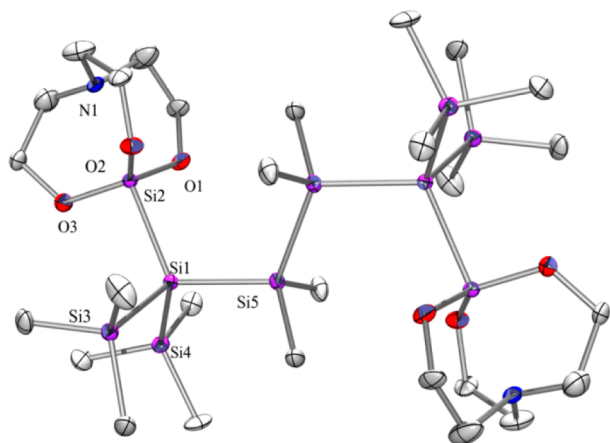


Figure 10. Molecular structure of **17** (thermal ellipsoid plot drawn at the 30% probability level). All hydrogen atoms are omitted for clarity. Selected bond lengths (in Å) and angles (in deg): Si(1)–Si(2) 2.3504(18), Si(2)–O(1) 1.657(4), Si(2)–N(1) 2.223(4), Si(3)–C(9) 1.872(7); O(2)–Si(2)–O(3) 117.5(2), N(1)–Si(2)–Si(1) 177.79(14), C(4)–N(1)–C(2) 115.2(6).

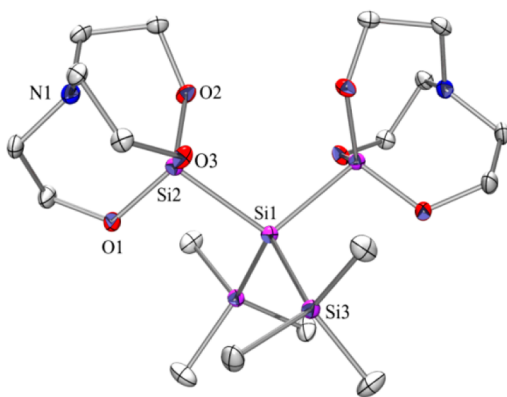


Figure 11. Molecular structure of **18** (thermal ellipsoid plot drawn at the 30% probability level). All hydrogen atoms are omitted for clarity. Selected bond lengths (in Å) and angles (in deg): Si(1)–Si(3) 2.3343(5), Si(1)–Si(2) 2.3416(5), Si(2)–O(2) 1.6512(10), Si(3)–C(9) 1.8728(15), N(1)–C(6) 1.4574(17), O(1)–C(1) 1.4232(17); Si(3)–Si(1)–Si(2) 108.594(17), O(2)–Si(2)–O(3) 116.47(5), C(6)–N(1)–C(2) 115.79(12), C(6)–N(1)–C(4) 115.73(11), C(2)–N(1)–C(4) 116.37(11).

Then again, in accordance with what was found by NMR spectroscopy for the geminal disilatrane **18**, the respective Si–N distance for **18** is 2.421(1) Å, being the longest of the neutral silatranyl oligosilanes, but still the Si–SiO₃ bond distance is in the same range as for all the other neutral compounds. For the protonated silatrane **19** no interaction between silicon and nitrogen can be detected; the Si–N distances for the three crystallographically independent molecules are around 3.39 Å (Table 2), which is even longer than those for the silanide cases of **10**, **11**, and **14**. Accordingly, the Si–SiO₃ bond distances are shortened (2.301(1)/2.304(1)/2.307(1) Å) to about the same extent that was detected for **10**, **11**, and **14**. The triflate counterions are situated above the silatrane close to the protonated nitrogen with H–O distances between 1.73(2) and 1.76(2) Å.

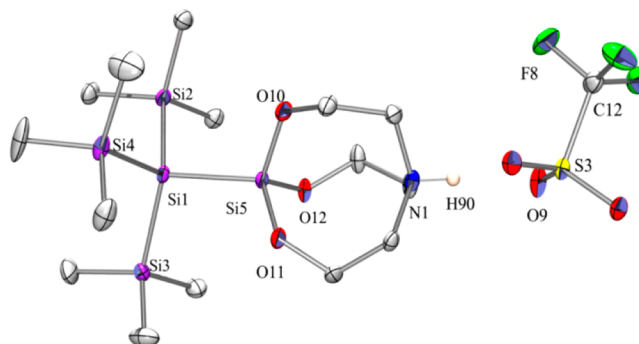


Figure 12. Molecular structure of **19** (thermal ellipsoid plot drawn at the 30% probability level). All hydrogen atoms are omitted for clarity. Selected bond lengths (in Å) and angles (in deg): Si(1)–Si(5) 2.3072(12), Si(1)–Si(3) 2.3439(13), Si(2)–C(26) 1.868(4), Si(5)–O(11) 1.637(2), N(1)–C(18) 1.503(4), O(9)–S(3) 1.447(2), O(10)–C(13) 1.414(4), S(3)–C(12) 1.824(4), F(8)–C(12) 1.338(4); Si(5)–Si(1)–Si(3) 105.74(5), Si(5)–Si(1)–Si(4) 107.83(5), O(11)–Si(5)–O(10) 106.94(12), C(18)–N(1)–C(16) 116.8(3).

CONCLUSION

Although silatrane is a substance class that has been known for some time, almost no examples exist with silyl substituents. Our interest in the chemistry and properties of oligosilanes led us to investigate possibilities to attach silatranyl units to oligosilanes. While reactions of potassium oligosilanides with chlorosilatrane did not give the expected compounds in satisfactory yields, it was found that analogous reactions with a silatranyl triflate give the oligosilanylated silatrane in acceptable yields.

²⁹Si NMR spectroscopy clearly suggests a Si–N interaction, as indicated by upfield-shifted SiO₃ resonances. In addition, the solid-state structures with Si–N distances between 2.29 and 2.16 Å are supportive of this. Weakening of the Si–Si bond trans to the Si–N interaction, however, becomes only obvious upon comparing the Si–Si distances of structurally related compounds with the Si–N interaction either active or “turned off” by protonation of the nitrogen lone pair. Accordingly, the weakening of the (Me₃Si)₃Si–Si bond by the silatrane effect accounts to an elongation of about 0.05 Å.

Attempts to submit the obtained oligosilanyl silatrane to further silanide formation by reaction with potassium *tert*-butoxide were successful. By single-crystal XRD analysis and multinuclear NMR spectroscopy it was found that upon silanide formation again the silatrane Si–N interaction is turned off. The obtained silanides can be used as building blocks for the construction of more extended oligosilane systems or for the preparation of a geminal disilatranyl silane.

EXPERIMENTAL SECTION

General Remarks. All reactions involving air-sensitive compounds were carried out under an atmosphere of dry nitrogen or argon using either Schlenk techniques or a glovebox. Reagent grade CHCl₃ was used for the synthesis of chlorosilatrane **1**. All other solvents were dried using a column-based solvent purification system.⁴⁷ Ethyltris(trimethylsilyl)silane,³¹ isopropyltris(trimethylsilyl)silane,⁴⁸ phenyltris(trimethylsilyl)silane,⁴⁸ 2,2-bis(trimethylsilyl)octamethyltetrasilane,⁴² (*tert*-butyldimethylsilyl)tris(trimethylsilyl)silane,³¹ 1-chloro-3,3-bis(trimethylsilyl)heptamethyltetrasilane,¹⁹ and 1,2-dichlorotetramethyldisilane^{49,50} were prepared according to previously published procedures. Methyltris(trimethylsilyl)silane⁵¹ was prepared similarly to ethyltris(trimethylsilyl)silane³¹ by reaction of tris(trimethylsilyl)silyl

Table 2. Compilation of Structural Data Derived by Single-Crystal XRD Analysis of 3, 5–7, 9–11, 14, and 17–19

compd	$d_{\text{Si-N}}$ (Å)	$d_{\text{Si-SiO}_3}$ (Å)	$d_{\text{Si-SiMe}_3}$ (Å)	$d_{\text{Si-R}}$ (Å)	$\angle_{\text{Me}_3\text{SiSiR}}$ (deg)
3	2.292(3)	2.351(2)	2.335(2)–2.341(2)		
5	2.283(2)	2.346(1)	2.341(1)–2.346(1)	2.351(3)	
6	2.167(3)	2.352(1)	2.339(1)/2.346(1)	1.908(3)	
7	2.182(4)	2.344(2)	2.334(2)/2.356(2)	1.907(5)	
9	2.162(5)	2.383(2)	2.342(2)–2.358(2)	1.904(6)/1.911(7)	
10	3.134(4)	2.308(2)	2.312(2)/2.318(2)	3.363(2)	103.42(7)
11	3.184(3)	2.295(1)	2.328(1)	2.339(1)/3.632(1)	104.65(5)
14	3.103(2)	2.3088(8)	2.3431(8)	1.914(2)/3.5722(8)	100.25(5)
17	2.223(4)/2.209(4)	2.350(2)/2.342(2)	2.343(2)–2.346(2)	2.358(2)–2.369(2)	
18	2.421(1)	2.3415(5)	2.3343(5)		
19	3.394(3)/3.389(3)/3.397(3)	2.301(1)/2.304(1)/2.307(1)	2.339(1)–2.351(1)		

potassium with dimethyl sulfate. All other chemicals were obtained from different suppliers and used without further purification.

^1H (300 MHz), ^{13}C (75.4 MHz), ^{19}F (282.2 MHz), and ^{29}Si (59.3 MHz) NMR spectra were recorded on a Varian INOVA 300 spectrometer and are referenced to tetramethylsilane (TMS) for ^1H , ^{13}C , and ^{29}Si and to CFCl_3 for ^{19}F . In the case of reaction samples a D_2O capillary was used to provide an external lock frequency signal. To compensate for the low isotopic abundance of ^{29}Si , the INEPT pulse sequence^{52,53} was used for the amplification of the signal. Elemental analysis was carried out using a Heraeus VARIO ELEMENTAR instrument. GC/MS analyses were carried out on a Agilent 7890A (capillary column HP-5MS; 30 m \times 0.250 mm; film 0.25 μm) with an Agilent 5975C mass spectrometer.

X-ray Structure Determination. For X-ray structure analyses the crystals were mounted onto the tip of glass fibers, and data collection was performed with a BRUKER-AXS SMART APEX CCD diffractometer using graphite-monochromated $\text{Mo K}\alpha$ radiation (0.71073 Å). The data were reduced to F_o^2 and corrected for absorption effects with SAINT⁵⁴ and SADABS,⁵⁵ respectively. The structures were solved by direct methods and refined by full-matrix least-squares methods (SHELXL97).⁵⁶ If not noted otherwise, all non-hydrogen atoms were refined with anisotropic displacement parameters and all hydrogen atoms were located in calculated positions to correspond to standard bond lengths and angles. Crystallographic data (excluding structure factors) for the structures of compounds 3, 5–7, 9–11, 14, and 17–19 reported in this paper have been deposited with the Cambridge Crystallographic Data Center as supplementary publication nos. CCDC 1062942 (3), 1062948 (5), 1062943 (6), 1062944 (7), 1062946 (9), 1062945 (10), 1062951 (11), 1062947 (14), 1062941(17), 1062949 (18), and 1062950 (19). Data can be obtained free of charge at <http://www.ccdc.cam.ac.uk/products/csd/request/>.

Figures of solid-state molecular structures were generated using Ortep-3 as implemented in WINGX⁵⁷ and rendered using POV-Ray 3.6.⁵⁸

$\text{N}(\text{CH}_2\text{CH}_2\text{OSiMe}_3)_3$. To a solution of triethanolamine (10.0 g, 0.067 mol) in dichloromethane (100 mL) in a 500 mL two-neck flask was added triethylamine (30.0 g, 0.301 mol), and the mixture was cooled to 0 °C in an ice bath. Within 1 h trimethylchlorosilane (25.5 g, 0.234 mol) was added dropwise to the flask. After the ice bath was removed, the reaction mixture was warmed to room temperature with stirring over 2 h. The reaction mixture was then added slowly to water (100 mL), and the organic phase was separated from the aqueous layer, which was washed twice with small portions of dichloromethane. The combined organic phases were dried over Na_2SO_4 . The organic solvent was removed under vacuum, and a pale yellow oil (18.0 g, 0.049 mol, 73%) was obtained as the product with spectroscopic properties in accordance with reported data.⁵⁹ NMR (δ ppm, CDCl_3): ^1H , 3.51 (t, J = 6.8 Hz, 6H, OCH_2), 2.59 (t, J = 6.8 Hz, 6H, NCH_2), 0.00 (s, 27H, SiMe_3); ^{13}C , 61.05 (OCH_2), 57.59 (NCH_2), –0.69 (Me_3Si); ^{29}Si , 17.6.

Silatranyl Chloride (1). A mixture of $\text{N}(\text{CH}_2\text{CH}_2\text{OSiMe}_3)_3$ (14.0 g, 0.0383 mol) and SiCl_4 (7.00 g, 0.0412 mol) was dissolved in

chloroform (40 mL) in a 250 mL three-neck flask with condenser. The reaction mixture was stirred and heated for 6 h to reflux. After all volatiles were removed under vacuum, the residue was washed with chloroform and 1-chlorosilatrane (7.10 g, 0.0339 mol, 82%) was obtained as a white powder with spectroscopic properties in accordance with reported data.⁶⁰ NMR (δ ppm, CDCl_3): ^1H , 3.97 (t, J = 5.9 Hz, 6H, OCH_2), 3.01 (t, J = 5.9 Hz, 6H, NCH_2); ^{29}Si , –85.9.

Silatranyl Triflate (2). A slurry of 1-chlorosilatrane (2.00 g, 9.54 mmol, 1.00 equiv) and trimethylsilyl triflate (4.24 g, 19.07 mmol, 2.00 equiv) in toluene (1 mL) was strongly stirred and heated for 72 h to 65 °C. The progress of the reaction was monitored by ^1H NMR spectroscopic analysis of the peaks of trimethylsilyl triflate and the formed trimethylchlorosilane. Compound 2 was obtained as an air-sensitive white powder (2.92 g, 9.50 mmol, 99%) after removing volatiles under vacuum. NMR (δ ppm, $\text{DMSO}-d_6$): ^1H , 3.84 (t, J = 5.9 Hz, 6H, OCH_2), 3.13 (t, J = 5.9 Hz, 6H, NCH_2); ^{13}C , 118.33 (q, J = 318 Hz, CF_3), 57.52 (OCH_2), 50.69 (NCH_2); ^{29}Si , –97.1; ^{19}F , –77.45. Anal. Calcd for $\text{C}_7\text{H}_{12}\text{F}_3\text{NO}_6\text{SSi}$ (323.31): C, 26.00; H, 3.74; N, 4.33; S, 9.92. Found: C, 25.73; H, 3.54; N, 4.20; S, 9.69.

Tris(trimethylsilyl)silatranylsilane (3). Tetrakis(trimethylsilyl)silane (2.00 g, 6.23 mmol) and KO^tBu (734 mg, 6.54 mmol) in THF (5 mL) were stirred for 14 h. After the formation of the organosilyl anion was confirmed by means of NMR spectroscopy, the solvent was removed and toluene was added (5 mL). To a solution of this compound was added a suspension of 2 (2.22 g, 6.85 mmol) in toluene (2 mL) dropwise within 2 h. After 12 h the precipitate was removed by filtration and washed with pentane (3 mL) and then the solvent was removed. After sublimation (40 °C, 1 mbar) and recrystallization with hexane colorless crystalline 3 (1.35 g, 51%) was obtained. Mp: 144–146 °C. NMR (δ ppm, CDCl_3): ^1H , 3.65 (t, J = 5.6 Hz, 6H, OCH_2), 2.72 (t, J = 5.6 Hz, 6H, NCH_2), 0.15 (s, 27H, Me_3Si); ^{13}C , 58.56 (OCH_2), 52.15 (NCH_2), 2.20 (Me_3Si); ^{29}Si , –9.9 (Me_3Si), –52.6 (SiO_3), –133.9 (Si_q). NMR (δ ppm, C_6D_6): ^1H , 3.30 (t, J = 5.6 Hz, 6H, OCH_2), 1.83 (t, J = 5.6 Hz, 6H, NCH_2), 0.53 (s, 27H, Me_3Si); ^{13}C , 58.55 (OCH_2), 51.53 (NCH_2), 2.77 (Me_3Si). Anal. Calcd for $\text{C}_{15}\text{H}_{39}\text{NO}_3\text{Si}_5$ (421.91): C, 42.70; H, 9.32; N, 3.32. Found: C, 43.29; H, 8.62; N, 3.25. MS (70 eV) m/z (%): 423(3) [$\text{M}^+ + \text{H}$], 406(4) [$\text{M}^+ - \text{Me}$], 278(3) [$(\text{SiMe}_3)_3\text{SiSiH}_3^+$], 249(1) [$(\text{SiMe}_3)_3\text{SiH}$], 232(2) [Si_4Me_8^+], 174(100) [$\text{N}(\text{CH}_2\text{CH}_2\text{O})_3\text{Si}^+$], 147(1) [$\text{N}(\text{CH}_2\text{CH}_2\text{O})_3^+$], 73(13) [SiMe_3^+].

1,1-Bis(trimethylsilyl)-1-silatranypentamethyltrisilane (4). The same procedure as for 9 was used, with 2,2-bis(trimethylsilyl)-octamethyltetrasilane (435 mg, 1.15 mmol), KO^tBu (135 mg, 1.21 mmol), and 2 (408 mg, 1.26 mmol). After recrystallization from diethyl ether/acetone/nitrile 1/1 colorless crystalline 4 (320 mg, 58%) was obtained. Mp: 78–79 °C. NMR (δ ppm, CDCl_3): ^1H , 3.66 (t, J = 5.6 Hz, 6H, OCH_2), 2.73 (t, J = 5.6 Hz, 6H, NCH_2), 0.19 (s, 6H, Me_3Si), 0.17 (s, 18H, $(\text{Me}_3\text{Si})_2\text{Si}$), 0.09 (s, 9H, Me_3Si); ^{13}C , 58.41 (OCH_2), 51.85 (NCH_2), 2.60 ($(\text{Me}_3\text{Si})_2\text{Si}$), –1.24 (Me_3Si), –2.01 (Me_2Si); ^{29}Si , –9.3 ($(\text{Me}_3\text{Si})_2\text{Si}$), –15.0 ($\text{Me}_3\text{Si-SiMe}_2$), –40.0 ($\text{Me}_3\text{Si-SiMe}_2$), –54.0 (SiO_3), –132.2 (Si_q). Anal. Calcd for $\text{C}_{17}\text{H}_{45}\text{NO}_3\text{Si}_6$ (480.06): C, 42.53; H, 9.45; N, 2.92. Found: C,

42.43; H, 8.94; N, 2.70. MS (70 eV) m/z (%): 464(10) [$M^+ - Me$], 406(100) [$M^+ - SiMe_3$], 290(3) [$Si_5C_{10}H_{30}^+$], 174(50) [$N(CH_2CH_2O)_3Si^+$], 131(3) [$NC_6H_{13}O_2^+$], 73(10) [$SiMe_3^+$]. UV: λ 223 nm ($\epsilon = 1.85 \times 10^4 \text{ M}^{-1} \text{ cm}^{-1}$).

(*tert*-Butyldimethylsilyl)bis(trimethylsilyl)silatranylsilane (5).

The same procedure as for 3 was used, with (*tert*-butyldimethylsilyl)tris(trimethylsilyl)silane (500 mg, 1.38 mmol), KO^tBu (162 mg, 1.45 mmol), and 2 (490 mg, 1.51 mmol). After recrystallization from hexane colorless crystalline 5 (268 mg, 42%) was obtained. Mp: 124–126 °C. NMR (δ ppm, $CDCl_3$): 1H , 3.65 (t, $J = 5.4$ Hz, 6H, OCH_2), 2.72 (t, $J = 5.4$ Hz, 6H, NCH_2), 0.93 (s, 9H, $(Me_3C)_3$), 0.18 (s, 18H, 2 Me_2Si), 0.12 (s, 6H, Me_2Si); ^{13}C , 58.68 (OCH_2), 52.09 (NCH_2), 27.98 (Me_3C), 18.43 (Me_3C), 2.77 (Me_3Si), -1.61 (Me_2Si); ^{29}Si , 4.0 ($tBuMe_2Si$), -9.7 (Me_3Si), -51.5 (SiO_3), -136.8 (Si_q). Anal. Calcd for $C_{18}H_{45}NO_3Si_5$ (463.99): C, 46.60; H, 9.78; N, 3.02. Found: C, 46.78; H, 8.99; N, 3.05. MS (70 eV) m/z (%): 463(3) [M^+], 448(8) [$M^+ - Me$], 406(15) [$M^+ - tBu$], 290(2) [$tBuSi_4Me_8H$], 174(100) [$N(CH_2CH_2O)_3Si^+$], 73(10) [$SiMe_3^+$].

Bis(trimethylsilyl)methylsilatranylsilane (6). The same procedure as for 3 was used, with methyltris(trimethylsilyl)silane (1.50 g, 5.70 mmol), KO^tBu (672 mg, 5.98 mmol), and 2 (2.03 g, 6.27 mmol). After sublimation (34 °C, 1 mbar) and recrystallization from hexane colorless crystalline 6 (1.16 g, 75%) was obtained. Mp: 109–111 °C. NMR (δ ppm, $CDCl_3$): 1H , 3.69 (t, $J = 5.6$ Hz, 6H, OCH_2), 2.74 (t, $J = 5.6$ Hz, 6H, NCH_2), 0.09 (s, 18H, 2 Me_3Si), 0.03 (s, 3H, $MeSi$); ^{13}C , 58.33 (OCH_2), 51.79 (NCH_2), -0.03 (2 Me_3Si), -12.66 ($MeSi$); ^{29}Si , -12.9 (Me_3Si), -57.8 (SiO_3), -88.0 ($SiMe$). Anal. Calcd for $C_{13}H_{33}NO_3Si_4$ (363.75): C, 42.93; H, 9.14; N, 3.85. Found: C, 43.20; H, 8.56; N, 3.72. MS (70 eV) m/z (%): 364(4) [M^+], 348(5) [$M^+ - Me$], 309(39) [$Me(SiMe_3)_2SiSiO_3C_3H_8^+$], 294(13) [$Me(SiMe_3)_2SiSiO_3C_2H_5^+$], 279(10) [$Me(SiMe_3)_2SiSiO_3CH_2^+$], 260(3) [$N(CH_2CH_2O)_3SiSi_2Me_2^+$], 193(5) [$Me_4Si_3O_3H^+$], 174(100) [$N(CH_2CH_2O)_3Si^+$], 132(3) [$Si_3O_3^+$], 73(9) [$SiMe_3^+$].

Bis(trimethylsilyl)ethylsilatranylsilane (7). The same procedure as for 3 was used, with ethyltris(trimethylsilyl)silane (600 mg, 2.17 mmol), KO^tBu (255 mg, 2.27 mmol), and 2 (772 mg, 2.39 mmol). After sublimation (38 °C, 1 mbar) and recrystallization from hexane colorless crystalline 7 (205 mg, 25%) was obtained. Mp: 109–111 °C. NMR (δ ppm, $CDCl_3$): 1H , 3.66 (t, $J = 5.6$ Hz, 6H, OCH_2), 2.71 (t, $J = 5.6$ Hz, 6H, NCH_2), 1.05 (t, $J = 7.9$ Hz, 3H, CH_2CH_3), 0.72 (q, $J = 7.3$ Hz, 2H, CH_2CH_3), 0.10 (s, 18H, 2 Me_3Si); ^{13}C , 58.34 (OCH_2), 51.86 (NCH_2), 12.79 (CH_2CH_3), 0.73 (2 Me_3Si), -0.02 (CH_2CH_3); ^{29}Si , -13.2 (Me_3Si), -56.6 (SiO_3), -78.4 ($SiEt$). Anal. Calcd for $C_{14}H_{35}NO_3Si_4$ 377.78: C, 44.51; H, 9.34; N, 3.71. Found: C, 44.96; H, 9.08; N, 3.57. MS (70 eV) m/z (%): 377(5) [M^+], 362(7) [$M^+ - Me$], 309(13) [$Et(SiMe_3)_2SiSiO_3C_2H_5^+$], 294(4) [$Et(SiMe_3)_2SiSiO_3CH_3^+$], 279(3) [$Et(SiMe_3)_2SiSiO_3^+$], 193(3) [$Me_4Si_3O_3H^+$], 174(100) [$N(CH_2CH_2O)_3Si^+$], 130(3) [$NC_6H_{12}O_2^+$], 73(7) [$SiMe_3^+$].

Bis(trimethylsilyl)isopropylsilatranylsilane (8). The same procedure as for 3 was used, with isopropyltris(trimethylsilyl)silane (500 mg, 1.28 mmol), KO^tBu (147 mg, 1.31 mmol), and 2 (453 mg, 1.40 mmol). After recrystallization from hexane colorless crystalline 8 (283 mg, 56%) was obtained. Mp: 118–120 °C. NMR (δ ppm, $CDCl_3$): 1H , 3.67 (t, $J = 5.6$ Hz, 6H, OCH_2), 2.73 (t, $J = 5.6$ Hz, 6H, NCH_2), 1.34 to 1.18 (m, 1H, CH), 1.12 (d, $J = 6.4$ Hz, 6H, Me_2CH), 0.14 (s, 18H, 2 Me_3Si); ^{13}C , 58.48 (OCH_2), 52.03 (NCH_2), 23.30 (Me_2CH), 11.05 (Me_2CH), 1.40 (Me_3Si); ^{29}Si , -13.5 (Me_3Si), -56.6 (SiO_3), -69.6 (Si^iPr). Anal. Calcd for $C_{15}H_{37}NO_3Si_4$ 391.19: C, 45.98; H, 9.52; N, 3.57. Found: C, 45.22; H, 8.98; N, 3.52. MS (70 eV) m/z (%): 391(5) [M^+], 376(7) [$M^+ - Me$], 202(2) [$^iPrSi_3Me_5^+$], 174(100) [$N(CH_2CH_2O)_3Si^+$], 130(2) [$NC_6H_{12}O_2^+$], 73(8) [$SiMe_3^+$].

Bis(trimethylsilyl)phenylsilatranylsilane (9). The same procedure as for 3 was used, with tris(trimethylsilyl)phenylsilane (2.00 g, 6.16 mmol), KO^tBu (712 mg, 6.34 mmol), and 2 (2.19 g, 6.77 mmol). After recrystallization using hexane colorless crystalline 9 (700 mg, 27%) was obtained. Mp: 161–163 °C. NMR (δ ppm, $CDCl_3$): 1H , 7.65 (m, 2H, Ph), 7.23 (m, 3H, Ph), 3.75 (t, $J = 5.6$ Hz, 6H, OCH_2), 2.76 (t, $J = 5.6$ Hz, 6H, NCH_2), 0.17 (s, 18H, 2 Me_3Si); ^{13}C , 136.91 (Ph), 129.07 (Ph), 127.03 (Ph), 126.40 (Ph), 58.14 (OCH_2), 51.62 (NCH_2), 0.54 (Me_3Si); ^{29}Si , -13.1 (Me_3Si), -56.6 (SiO_3), -76.2

(Si_q). Anal. Calcd for $C_{18}H_{35}NO_3Si_4$ 425.82: C, 50.77; H, 8.28; N, 3.29. Found: C, 49.84; H, 7.86; N, 3.19. MS (70 eV) m/z (%): 425(4) [M^+], 410(4) [$M^+ - Me$], 352(2) [$M^+ - SiMe_3$], 309(11) [$(SiMe_3)_2SiSiO_3C_4H_{11}^+$], 279(3) [$(SiMe_3)_2SiSiO_3C_2H_5^+$], 253(4) [$(SiMe_3)_2SiSiO_3H_3^+$], 193(2) [$Me_4Si_3O_3H^+$], 174(100) [$N(CH_2CH_2O)_3Si^+$], 135(6) [$Si_3O_3H_3^+$], 73(3) [$SiMe_3^+$].

Bis(trimethylsilyl)silatranylsilyl Potassium 18-Crown-6 (10).

A solution of 3 (50 mg, 0.12 mmol), KO^tBu (14 mg, 0.12 mmol), and 18-crown-6 (33 mg, 0.12 mmol) in benzene (1 mL) was stirred. After 14 h NMR spectroscopic analysis showed full conversion to 10. By addition of benzene (1 mL) pale orange crystals (77 mg, >99%) suitable for X-ray analysis could be obtained. NMR (δ ppm, C_6D_6): 1H , 3.86 (t, $J = 5.1$ Hz, 6H, OCH_2), 3.30 (s, 24H, 18-cr-6), 2.84 (t, $J = 5.1$ Hz, 6H, NCH_2), 0.78 (s, 18H, 2 Me_3Si); ^{13}C , 70.23 (18-cr-6), 60.96 (OCH_2), 54.26 (NCH_2), 7.18 (Me_3Si); ^{29}Si , -3.2 (Me_3Si), -11.8 (SiO_3), -210.5 (Si_q). MS (70 eV) m/z (%) (after treatment with ethyl bromide): 377(6) [M^+], 362(8) [$M^+ - Me$], 304(3) [$M^+ - SiMe_3$], 174(100) [$N(CH_2CH_2O)_3Si^+$], 130(3) [$NC_6H_{12}O_2^+$], 73(6) [$SiMe_3^+$].

(*tert*-Butyldimethylsilyl)trimethylsilylsilatranylsilyl Potassium 18-Crown-6 (11).

The same procedure as for 10 was used, with 5 (50 mg, 0.107 mmol), KO^tBu (13 mg, 0.133 mmol), and 18-crown-6 (30 mg, 0.113 mmol). After crystallization using heptane pale yellow crystalline 11 (74 mg, >99%) was obtained. NMR (δ ppm, C_6D_6): 1H , 3.81 (t, $J = 5.0$ Hz, 6H, OCH_2), 3.28 (s, 24H, CH_2O), 2.82 (t, $J = 5.0$ Hz, 6H, NCH_2), 1.19 (s, 9H, $(CH_3)_3C$), 0.71 (s, 9H, $(CH_3)_3Si$), 0.70 (s, 6H, $(CH_3)_2Si$); ^{13}C , 70.06 (18-cr-6), 60.97 (OCH_2), 54.23 (NCH_2), 29.22 (Me_3C), 19.22 (Me_3C), 7.37 ($(Me_3Si)Si$), 1.95 ($(Me_2Si)Si$); ^{29}Si , 11.3 ($tBuMe_2Si$), -3.0 (Me_3Si), -11.0 (SiO_3), -215.7 ($(Me_3Si)Si$). MS (70 eV) m/z (%) (after treatment with ethyl bromide): 419(3) [M^+], 404(6) [$M^+ - Me$], 362(22) [$M^+ - tBu$], 246(3) [$Si_3C_{11}H_{30}^+$], 174(100) [$N(CH_2CH_2O)_3Si^+$], 130(3) [$NC_6H_{12}O_2^+$], 73(8) [$SiMe_3^+$].

Trimethylsilylmethylsilatranylsilyl Potassium 18-Crown-6 (12).

A solution of 6 (200 mg, 0.55 mmol), KO^tBu (63 mg, 0.56 mmol), and 18-crown-6 (150 mg, 0.56 mmol) in C_6D_6 (2 mL) was stirred. After 14 h observation by NMR spectroscopy showed a mixture of the three products 12, bis(trimethylsilyl)methylsilyl potassium.18-crown-6, and $N(CH_2CH_2O)_3SiO^tBu$. 12: NMR (δ ppm, C_6D_6): 1H , 3.76 (t, $J = 4.4$ Hz, 6H, OCH_2), 3.26 (s, 24H, 18-cr-6), 2.80 (t, $J = 4.4$ Hz, 6H, NCH_2), 0.52 (s, 9H, Me_3Si), 0.45 (s, 3H, $MeSi$); ^{13}C , 70.03 (CH_2O), 60.91 (OCH_2), 54.17 (NCH_2), 4.06 (Me_3SiSi), -9.24 (CH_3Si); ^{29}Si , -5.1 (Me_3Si), -14.9 (SiO_3), -144.0 (Si_q). MS (70 eV) m/z (%) (after treatment with ethyl bromide): 318(1) [$M^+ - H$], 304(10) [$M^+ - Me$], 290(3) [$M^+ - Et$], 276(3) [$N(CH_2CH_2O)_3SiSi_2C_3H_{10}^+$], 246(10) [$M^+ - SiMe_3$], 218(41) [$N(CH_2CH_2O)_3SiSiCH_4^+$], 193(8) [$Me_4Si_3O_3H^+$], 174(100) [$N(CH_2CH_2O)_3Si^+$], 149(4) [$NC_6H_{15}O_3^+$], 130(4) [$NC_6H_{12}O_2^+$], 73(7) [$SiMe_3^+$].

Trimethylsilylethylsilatranylsilyl Potassium 18-Crown-6 (13).

A solution of 7 (50 mg, 0.13 mmol), KO^tBu (15 mg, 0.14 mmol), and 18-crown-6 (36 mg, 0.14 mmol) in benzene (1 mL) was stirred. After 14 h observation by NMR spectroscopy showed conversion to the three products 13, bis(trimethylsilyl)ethylsilyl potassium 18-crown-6, and $N(CH_2CH_2O)_3SiO^tBu$. 13: NMR (δ ppm, C_6D_6): 1H , 3.88 (t, $J = 5.2$ Hz, 6H, OCH_2), 3.27 (s, 24H, 18-cr-6), 2.88 (t, $J = 5.2$ Hz, 6H, NCH_2), 1.68 (t, $J = 7.5$ Hz, 3H), 1.41 (q, $J = 7.8$ Hz, 2H), 0.74 (s, 9H, Me_3Si); ^{13}C , 70.08 (CH_2O), 60.95 (OCH_2), 54.29 (NCH_2), 19.42 (CH_3CH_2), 4.85 (Me_3SiSi), 2.68 (CH_3CH_2); ^{29}Si , -6.2 (Me_3Si), -15.0 (SiO_3), -125.1 (Si_q). MS (70 eV) m/z (%) (after treatment with ethyl bromide): 333(1) [M^+], 318(8) [$M^+ - Me$], 304(4) [$M^+ - Et$], 290(3) [$N(CH_2CH_2O)_3SiSi_2Me_4^+$], 276(3) [$N(CH_2CH_2O)_3SiSi_2C_3H_{10}^+$], 260(11) [$M^+ - SiMe_3$], 246(3) [$N(CH_2CH_2O)_3SiSiC_3H_8^+$], 232(42) [$N(CH_2CH_2O)_3SiSiC_2H_6^+$], 218(2) [$N(CH_2CH_2O)_3SiSiCH_4^+$], 204(3) [$N(CH_2CH_2O)_3SiSiH_2^+$], 174(100) [$N(CH_2CH_2O)_3Si^+$], 130(4) [$NC_6H_{12}O_2^+$], 73(5) [$SiMe_3^+$].

Trimethylsilylphenylsilatranylsilyl Potassium 18-Crown-6 (14).

A solution of 9 (50 mg, 0.12 mmol), KO^tBu (14 mg, 0.12 mmol), and 18-crown-6 (32 mg, 0.12 mmol) in benzene (1 mL) was

stirred. After 14 h observation by NMR spectroscopy showed quantitative conversion to **14**. By addition of benzene (1 mL) yellow crystals (77 mg, >99%) suitable for X-ray analysis were obtained. NMR (δ ppm, C_6D_6): 1H , 8.13 (d, 2H, Ph), 7.02 (m, 3H), 3.84 (t, J = 5.0 Hz, 6H, OCH_2), 3.20 (s, 24H, CH_3O), 2.81 (t, J = 5.0 Hz, 6H, NCH_2), 0.69 (s, 9H, Me_3Si); ^{13}C , 157.75 (Ph), 137.61 (Ph), 126.19 (Ph), 121.69 (Ph), 70.15 (18-cr-6), 61.14 (OCH_2), 54.17 (NCH_2), 4.58 (Me_3Si); ^{29}Si , -7.7 (Me_3Si), -19.4 (SiO_3), -113.0 (Si_4). MS (70 eV) m/z (%) (after treatment with ethyl bromide): 366(5) [$M^+ - Me$], 308(10) [$M^+ - SiMe_3$], 280(31) [$N(CH_2CH_2O)_3SiSiPhH^+$], 253(4) [$PhSi_3O_3C_3H_8^+$], 174(100) [$N(CH_2CH_2O)_3Si^+$], 135(7) [$Si_3O_3H_3^+$], 73(3) [$SiMe_3^+$].

2,5,5-Tris(trimethylsilyl)-2-silatranyldecamethylhexasilane (16). **3** (350 mg, 0.75 mmol) and KO^tBu (87 mg, 0.77 mmol) were dissolved in THF (2 mL). After 14 h the formation of the silyl anion **10** was confirmed by means of NMR spectroscopy; the solvent was removed, and benzene was added (3 mL). This solution was added dropwise to 1-chloro-3,3-bis(trimethylsilyl)heptamethyltetrasilane (300 mg, 0.75 mmol) in toluene (3 mL) at 0 °C within 1 h. After 12 h the solvent was removed, the residue treated with pentane, and the insoluble parts were filtered off. The solvent was again removed, and recrystallization with diethyl ether/acetonitrile (1/1) afforded colorless crystalline **16** (354 mg, 66%). Mp: 130–136 °C. NMR (δ ppm, $CDCl_3$): 1H , 3.66 (t, J = 5.56 Hz, 6H, OCH_2), 2.73 (t, J = 5.61 Hz, 6H, NCH_2), 0.39 (s, 6H, Me_2Si), 0.35 (s, 6H, Me_2Si), 0.24 (s, 27H, 3 Me_3Si), 0.20 (s, 18H, 2 Me_3Si); ^{13}C , 58.50 (OCH_2), 51.84 (NCH_2), 3.52 (Me_3Si), 2.97 (Me_3Si), 0.53 (Me_2Si), 0.40 (Me_2Si); ^{29}Si , -9.2 (Me_3Si), -9.6 (Me_3Si), -30.6 (Me_2Si), -30.8 (Me_2Si), -53.8 (SiO_3), -128.6 (Si_4), -129.3 (Si_4). Anal. Calcd for $C_{25}H_{69}NO_3Si_{10}$ (712.68): C, 42.13; H, 9.76; N, 1.97. Found: C, 41.66; H, 9.65; N, 1.73. UV: λ 254 nm (ϵ = 5.45×10^4 M $^{-1}$ cm $^{-1}$).

2,5-Bis(trimethylsilyl)-2,5-disilatranyldecamethylhexasilane (17). The same procedure as for **3** was used, with **3** (500 mg, 1.19 mmol), KO^tBu (137 mg, 1.22 mmol), and dichlorotetramethyldisilane (116 mg, 0.62 mmol). Recrystallization with diethyl ether/acetonitrile (1/1) afforded colorless crystalline **17** (200 mg, 41%). Mp: 244–248 °C. NMR (δ ppm, C_6D_6): 1H , 3.36 (t, J = 5.6 Hz, 12H, OCH_2), 1.90 (t, J = 5.6 Hz, 12H, NCH_2), 0.84 (s, 12H, $(CH_3)_2Si$), 0.61 (s, 36H, $(CH_3)_3Si$); ^{13}C , 58.75 (OCH_2), 51.49 (NCH_2), 3.54 ($(Me_3Si)_2Si$), 0.56 (Me_2Si); ^{29}Si , -9.2 ($(Me_3Si)_3Si$), -31.2 (Me_2Si), -53.2 (SiO_3), -129.5 ($(Me_3Si)_3Si$). MS (70 eV) m/z (%): 799(1) [$M^+ - Me$], 640(1) [$N(CH_2CH_2O)_3SiSi_8O_3C_{13}H_{38}^+$], 464(11) [$N(CH_2CH_2O)_3SiSi_5C_{10}H_{30}^+$], 406(100) [$N(CH_2CH_2O)_3SiSi_4C_8H_{24}^+$], 362(3) [$N(CH_2CH_2O)_3SiSi_4C_5H_{16}^+$], 278(3) [$(SiMe_3)_2SiSiO_3C_2H_4^+$], 246(2) [$Si_4O_3C_6H_{14}^+$], 207(7) [$Si_4O_3C_3H_{11}^+$], 174(32) [$N(CH_2CH_2O)_3Si^+$], 117(3) [$NC_5H_{11}O_2^+$], 73(10) [$SiMe_3^+$]. Anal. Calcd for $C_{28}H_{72}N_2O_6Si_{10}$ (813.74): C, 41.33; H, 8.92; N, 3.44. Found: C, 41.27; H, 8.22; N, 3.28. UV: λ 252 nm (ϵ = 7.48×10^4 M $^{-1}$ cm $^{-1}$).

Bis(trimethylsilyl)disilatranylsilane (18). The same procedure as for **6** was used, with **3** (310 mg, 0.73 mmol), KO^tBu (85 mg, 1.03 mmol), and **2** (261 mg, 0.81 mmol). After recrystallization with pentane colorless crystalline **6** (90 mg, 23%) was obtained. Mp: 138–140 °C. NMR (δ ppm, $CDCl_3$): 1H , 3.68 (t, J = 5.4 Hz, 12H, OCH_2), 2.71 (t, J = 5.4 Hz, 12H, NCH_2), 0.17 (s, 18H, 2 Me_3Si); ^{13}C , 59.38 (OCH_2), 52.71 (NCH_2), 1.72 (Me_3Si); ^{29}Si , -9.5 (Me_3Si), -46.8 (SiO_3), -135.5 (Si_4). Anal. Calcd for $C_{18}H_{42}N_2O_6Si_5$ (522.97): C, 41.34; H, 8.10; N, 5.36. Found: C, 42.56; H, 7.38; N, 5.28. MS (70 eV) m/z (%): 522(3) [M^+], 507(6) [$M^+ - Me$], 449(6) [$M^+ - SiMe_3$], 393(1) [$N(CH_2CH_2O)_3SiSi_3O_3C_6H_{15}^+$], 347(17) [$N(CH_2CH_2O)_3SiSi_3C_6H_{17}^+$], 309(13) [$(SiMe_3)_2SiSiO_3C_4H_{11}^+$], 279(3) [$(SiMe_3)_2SiSiO_3C_2H_5^+$], 248(3) [$Si_4O_3C_6H_{16}^+$], 218(11) [$Si_4O_3C_4H_{10}^+$], 174(100) [$N(CH_2CH_2O)_3Si^+$], 130(6) [$NC_6H_{12}O_2^+$], 73(5) [$SiMe_3^+$].

Tris(trimethylsilyl)silatranyliumsilane Triflate (19-OTf). To an ice-cold solution of **3** (93 mg, 0.22 mmol) in toluene (1 mL) was added triflic acid (31 mg, 0.21 mmol in 1 mL of toluene) dropwise. After 3 h the solvent was removed and crystallization from benzene afforded colorless crystalline **19-OTf** (84 mg, 0.15 mmol, 67%). Mp: 156–160 °C. NMR (δ ppm, C_6D_6): 1H , 10.68 (s, 1H, NH), 3.34 (s,

6H, OCH_2), 2.64 (s, 6H, NCH_2), 0.25 (s, 27H, $(Me_3)_3Si$); ^{13}C , 121.52 (q, J = 319 Hz, CF_3), 56.44 (OCH_2), 53.13 (NCH_2), 2.11 (Me_3Si); ^{29}Si , -9.7 (Me_3Si), -22.8 (SiO_3), -141.1 ($(Me_3Si)_2Si$); ^{19}F , -77.85.

Tris(trimethylsilyl)silatranyliumsilane Trichloroacetate (19-TCA). To a solution of **3** (30 mg, 0.07 mmol) in C_6D_6 (0.5 mL) was added trichloroacetic acid (60 mg, 0.37 mmol). 1H NMR spectroscopic monitoring showed quantitative conversion to **19-TCA**. NMR (δ ppm, C_6D_6): 1H , 10.73 (bs, SH, NH and Cl_3CCO_2H), 3.49 (s, 6H, OCH_2), 2.72 (s, 6H, NCH_2), 0.26 (s, 27H, $(Me_3)_3Si$); ^{29}Si , -9.7 (Me_3Si), -23.2 (SiO_3), -141.1 ($(Me_3Si)_2Si$).

■ ASSOCIATED CONTENT

Supporting Information

Tables, figures, and CIF files containing crystallographic information for compounds **3**, **5–7**, **9–11**, **14**, and **17–19** and NMR spectra for **9–14**, **18**, and **19**. The Supporting Information is available free of charge on the ACS Publications website at DOI: 10.1021/acs.organomet.5b00404.

■ AUTHOR INFORMATION

Corresponding Author

*E-mail for C.M.: christoph.marschner@tugraz.at.

Author Contributions

The manuscript was written through contributions of all authors. All authors have given approval to the final version of the manuscript.

Notes

The authors declare no competing financial interest.

■ ACKNOWLEDGMENTS

Support for this study was provided by the Austrian Fonds zur Förderung der wissenschaftlichen Forschung (FWF) via the project P-26417 (C.M.).

■ REFERENCES

- (1) Vollhardt, K. P. C. *Organische Chemie*, 3rd ed.; Wiley-VCH: Weinheim, Germany, 2000.
- (2) Carey, F. A.; Sundberg, R. J. *Advanced Organic Chemistry. Part A: Structure and Mechanisms*, 5th ed.; Springer: Berlin, 2008 (corr. 2nd printing).
- (3) A recent explanation for the differences of carbon and silicon with respect to hypercoordination is given in: Pierrefixe, S. C. A. H.; Fonseca Guerra, C.; Bickelhaupt, F. M. *Chem. - Eur. J.* **2008**, *14*, 819–828.
- (4) Puri, J. K.; Singh, R.; Chahal, V. K. *Chem. Soc. Rev.* **2011**, *40*, 1791.
- (5) Pestunovich, V.; Kirpichenko, S.; Voronkov, M. In *The Chemistry of Organic Silicon Compounds*; Rappoport, Z., Apeloig, Y., Eds.; Wiley: Chichester, U.K., 2003; pp 1447–1537.
- (6) Kost, D.; Kalikhman, I. In *The Chemistry of Organic Silicon Compounds*; Rappoport, Z., Apeloig, Y., Eds.; Wiley: Chichester, U.K., 2003; pp 1339–1445.
- (7) Selina, A.; Karlov, S.; Zaitseva, G. *Chem. Heterocycl. Compd.* **2006**, *42*, 1518–1556.
- (8) Verkade, J. G. *Coord. Chem. Rev.* **1994**, *137*, 233–295.
- (9) Karlov, S. S.; Zaitseva, G. S. *Chem. Heterocycl. Compd.* **2001**, *37*, 1325–1357.
- (10) Varga, R. A.; Rotar, A.; Schürmann, M.; Jurkschat, K.; Silvestru, C. *Eur. J. Inorg. Chem.* **2006**, *2006*, 1475–1486.
- (11) Theddu, N.; Vedejs, E. *J. Org. Chem.* **2013**, *78*, 5061–5066.
- (12) Jurkschat, K.; Pieper, N.; Seemeyer, S.; Schürmann, M.; Biesemans, M.; Verbruggen, I.; Willem, R. *Organometallics* **2001**, *20*, 868–880.
- (13) Yamamoto, Y.; Matsubara, H.; Murakami, K.; Yorimitsu, H.; Osuka, A. *Chem. - Asian J.* **2015**, *10*, 219–224.

- (14) Singh, G.; Saroa, A.; Garg, M.; Sharma, R. P.; Gubanov, A. I.; Smolentsev, A. I. *J. Organomet. Chem.* **2012**, *719*, 21–25.
- (15) Zaitsev, K. V.; Churakov, A.; Poleshchuk, O. K.; Yuri, O. F.; Zaitseva, G. S.; Karlov, S. S. *Dalton Trans.* **2014**, *43*, 6605–6609.
- (16) Wallner, A.; Emanuelsson, R.; Baumgartner, J.; Marschner, C.; Ottosson, H. *Organometallics* **2013**, *32*, 396–405.
- (17) Wallner, A.; Hlina, J.; Wagner, H.; Baumgartner, J.; Marschner, C. *Organometallics* **2011**, *30*, 3930–3938.
- (18) Wallner, A.; Hlina, J.; Konopa, T.; Wagner, H.; Baumgartner, J.; Marschner, C.; Flörke, U. *Organometallics* **2010**, *29*, 2660–2675.
- (19) Wallner, A.; Wagner, H.; Baumgartner, J.; Marschner, C.; Rohm, H. W.; Kockerling, M.; Krempner, C. *Organometallics* **2008**, *27*, S221–S229.
- (20) Marschner, C.; Baumgartner, J.; Wallner, A. *Dalton Trans.* **2006**, 5667–5674.
- (21) Michl, J.; West, R. *Acc. Chem. Res.* **2000**, *33*, 821–823.
- (22) Koe, J. R.; Motonaga, M.; Fujiki, M.; West, R. *Macromolecules* **2001**, *34*, 706–712.
- (23) Jäger-Fiedler, U.; Köckerling, M.; Reinke, H.; Krempner, C. *Chem. Commun.* **2010**, *46*, 4535–4537.
- (24) Krempner, C.; Ludwig, R.; Flemming, A.; Miethchen, R.; Köckerling, M. *Chem. Commun.* **2007**, 1810–1812.
- (25) Jäger-Fiedler, U.; Köckerling, M.; Ludwig, R.; Wulf, A.; Krempner, C. *Angew. Chem., Int. Ed.* **2006**, *45*, 6755–6759.
- (26) Krempner, C.; Kopf, J.; Mamat, C.; Reinke, H.; Spannenberg, A. *Angew. Chem., Int. Ed.* **2004**, *43*, S406–S408.
- (27) El-Sayed, I.; Hatanaka, Y.; Muguruma, C.; Shimada, S.; Tanaka, M.; Koga, N.; Mikami, M. *J. Am. Chem. Soc.* **1999**, *121*, 5095–5096.
- (28) El-Sayed, I.; Hatanaka, Y.; Onozawa, S.; Tanaka, M. *J. Am. Chem. Soc.* **2001**, *123*, 3597–3598.
- (29) Adamovich, S. N.; Prokopyev, V. Y.; Rakhlin, V. I.; Mirskov, R. G.; Voronkov, M. G. *Synth. React. Inorg. Met.-Org. Chem.* **1991**, *21*, 1261–1264.
- (30) Karlov, S. S.; Shutov, P. L.; Akhmedov, N. G.; Seip, M. A.; Lorberth, J.; Zaitseva, G. S. *J. Organomet. Chem.* **2000**, *598*, 387–394.
- (31) Marschner, C. *Eur. J. Inorg. Chem.* **1998**, *1998*, 221–226.
- (32) Kayser, C.; Marschner, C. *Monatsh. Chem.* **1999**, *130*, 203–206.
- (33) Kayser, C.; Kickelbick, G.; Marschner, C. *Angew. Chem., Int. Ed.* **2002**, *41*, 989–992.
- (34) Gaderbauer, W.; Balatoni, I.; Wagner, H.; Baumgartner, J.; Marschner, C. *Dalton Trans.* **2010**, *39*, 1598.
- (35) Yoshikawa, A.; Gordon, M. S.; Sidorkin, V. F.; Pestunovich, V. A. *Organometallics* **2001**, *20*, 927–931.
- (36) Garant, R. J.; Daniels, L. M.; Das, S. K.; Janakiraman, M. N.; Jacobson, R. A.; Verkade, J. G. *J. Am. Chem. Soc.* **1991**, *113*, 5728–5735.
- (37) The Evans Group/pKa_table: http://www2.lsddiv.harvard.edu/pdf/evans_pKa_table.pdf (accessed June 15, 2015).
- (38) Attar-Bashi, M. T.; Rickard, C. E. F.; Roper, W. R.; Wright, L. J.; Woodgate, S. D. *Organometallics* **1998**, *17*, 504–506.
- (39) Rickard, C. E. F.; Roper, W. R.; Woodgate, S. D.; Wright, L. J. *J. Organomet. Chem.* **2000**, *609*, 177–183.
- (40) Marsmann, H.; Raml, W.; Hengge, E. Z. *Naturforsch., B: J. Chem. Sci.* **1980**, *35*, 1541–1547.
- (41) Jenkins, D. M.; Teng, W.; Englich, U.; Stone, D.; Ruhlandt-Senge, K. *Organometallics* **2001**, *20*, 4600–4606.
- (42) Whittaker, S. M.; Brun, M.-C.; Cervantes-Lee, F.; Pannell, K. H. *J. Organomet. Chem.* **1995**, *499*, 247–252.
- (43) Miller, R. D.; Michl, J. *Chem. Rev.* **1989**, *89*, 1359–1410.
- (44) Likhar, P. R.; Zirngast, M.; Baumgartner, J.; Marschner, C. *Chem. Commun.* **2004**, 1764.
- (45) Krempner, C.; Chisholm, M. H.; Gallucci, J. *Angew. Chem., Int. Ed.* **2008**, *47*, 410–413.
- (46) Li, H.; Hope-Weeks, L. J.; Krempner, C. *Chem. Commun.* **2011**, *47*, 4117–4119.
- (47) Pangborn, A. B.; Giardello, M. A.; Grubbs, R. H.; Rosen, R. K.; Timmers, F. J. *Organometallics* **1996**, *15*, 1518–1520.
- (48) Kayser, C.; Fischer, R.; Baumgartner, J.; Marschner, C. *Organometallics* **2002**, *21*, 1023–1030.
- (49) Ishikawa, M.; Kumada, M.; Sakurai, H. *J. Organomet. Chem.* **1970**, *23*, 63–69.
- (50) Marschner, C.; Baumgartner, J. In *Science of Synthesis: Houben-Weyl Methods of Molecular Transformations*; Oestreich, M., Ed.; Thieme: Stuttgart, Germany, 2013.
- (51) Gilman, H.; Holmes, J. M.; Smith, C. L. *Chem. Ind.* **1965**, 848–849.
- (52) Morris, G. A.; Freeman, R. J. *Am. Chem. Soc.* **1979**, *101*, 760–762.
- (53) Helmer, B. J.; West, R. *Organometallics* **1982**, *1*, 877–879.
- (54) SAINTPLUS: *Software Reference Manual, Version 6.45*; Bruker-AXS: Madison, WI, 1997–2003.
- (55) Sheldrick, G. M. *SADABS, Version 2.10*; Bruker AXS, Madison, WI, 2003.
- (56) Sheldrick, G. M. *Acta Crystallogr., Sect. A: Found. Crystallogr.* **2008**, *64*, 112–122.
- (57) Farrugia, L. J. *J. Appl. Crystallogr.* **2012**, *45*, 849–854.
- (58) POVray 3.6; Persistence of Vision Pty. Ltd., 2004; retrieved from <http://www.povray.org/download/>.
- (59) Kupče, E.; Liepiņš, E.; Lapsina, A.; Zelchan, G.; Lukevics, E. J. *Organomet. Chem.* **1983**, *251*, 15–29.
- (60) Bellama, J. M.; Nies, J. D.; Ben-Zvi, N. *Magn. Reson. Chem.* **1986**, *24*, 748–753.